

## Selecting Targets for Molecular Imaging of Gastric Cancer An Immunohistochemical Evaluation

Houvast, Ruben D.; van Duijvenvoorde, Maurice; Thijse, Kira; de Steur, Wobbe O.; de Geus-Oei, Lioe Fee; Crobach, A. Stijn L.P.; Burggraaf, Jacobus; Vahrmeijer, Alexander L.; Kuppen, Peter J.K.

**DOI**

[10.1007/s40291-024-00755-5](https://doi.org/10.1007/s40291-024-00755-5)

**Publication date**

2024

**Document Version**

Final published version

**Published in**

Molecular Diagnosis and Therapy

**Citation (APA)**

Houvast, R. D., van Duijvenvoorde, M., Thijse, K., de Steur, W. O., de Geus-Oei, L. F., Crobach, A. S. L. P., Burggraaf, J., Vahrmeijer, A. L., & Kuppen, P. J. K. (2024). Selecting Targets for Molecular Imaging of Gastric Cancer: An Immunohistochemical Evaluation. *Molecular Diagnosis and Therapy*, 29 (2025)(2), 213-227. <https://doi.org/10.1007/s40291-024-00755-5>

**Important note**

To cite this publication, please use the final published version (if applicable).  
Please check the document version above.

**Copyright**

Other than for strictly personal use, it is not permitted to download, forward or distribute the text or part of it, without the consent of the author(s) and/or copyright holder(s), unless the work is under an open content license such as Creative Commons.

**Takedown policy**

Please contact us and provide details if you believe this document breaches copyrights.  
We will remove access to the work immediately and investigate your claim.



# Selecting Targets for Molecular Imaging of Gastric Cancer: An Immunohistochemical Evaluation

Ruben D. Houvast<sup>1</sup> · Maurice van Duijvenvoorde<sup>1</sup> · Kira Thijse<sup>1</sup> · Wobbe O. de Steur<sup>1</sup> · Lioe-Fee de Geus-Oei<sup>2,3,4</sup> · A. Stijn. L. P. Crobach<sup>5</sup> · Jacobus Burggraaf<sup>1,6</sup> · Alexander L. Vahrmeijer<sup>1</sup> · Peter J. K. Kuppen<sup>1</sup>

Accepted: 23 October 2024  
© The Author(s) 2024

## Abstract

**Purpose** Tumor-targeted positron emission tomography (PET) and fluorescence-guided surgery (FGS) could address current challenges in pre- and intraoperative imaging of gastric cancer. Adequate selection of molecular imaging targets remains crucial for successful tumor visualization. This study evaluated the potential of integrin  $\alpha_v\beta_6$ , carcinoembryonic antigen-related cell adhesion molecule 5 (CEACAM5), epidermal growth factor receptor (EGFR), epithelial cell adhesion molecule (EpCAM) and human epidermal growth factor receptor-2 (HER2) for molecular imaging of primary gastric cancer, as well as lymph node and distant metastases.

**Methods** Expression of  $\alpha_v\beta_6$ , CEACAM5, EGFR, EpCAM and HER2 was determined using immunohistochemistry in human tissue specimens of primary gastric adenocarcinoma, healthy surrounding stomach, esophageal and duodenal tissue, tumor-positive and tumor-negative lymph nodes, and distant metastases, followed by quantification using the total immunostaining score (TIS).

**Results** Positive biomarker expression in primary gastric tumors was observed in 86% for  $\alpha_v\beta_6$ , 72% for CEACAM5, 77% for EGFR, 93% for EpCAM and 71% for HER2. Tumor expression of CEACAM5, EGFR and EpCAM was higher compared to healthy stomach tissue expression, while this was not the case for  $\alpha_v\beta_6$  and HER2. Tumor-positive lymph nodes could be distinguished from tumor-negative lymph nodes, with accuracy ranging from 82 to 93% between biomarkers. CEACAM5, EGFR and EpCAM were abundantly expressed on distant metastases, with expression in 88–95% of tissue specimens.

**Conclusion** Our findings show that CEACAM5, EGFR and EpCAM are promising targets for molecular imaging of primary gastric cancer, as well as visualization of both lymph node and distant metastases. Further clinical evaluation of PET and FGS tracers targeting these antigens is warranted.

## Key Points

Carcinoembryonic antigen-related cell adhesion molecule 5 (CEACAM5), epidermal growth factor receptor (EGFR) and epithelial cell adhesion molecule (EpCAM) are promising targets for molecular imaging of primary gastric cancer, as well as lymph node and distant metastases.

This study forms the preclinical groundwork for further clinical evaluation of positron emission tomography (PET) imaging and fluorescence-guided surgery tracers directed against these targets, which could enhance pre- and intraoperative imaging of gastric cancer and, ultimately, patient outcomes.

✉ Ruben D. Houvast  
R.D.Houvast@lumc.nl

<sup>1</sup> Department of Surgery, Leiden University Medical Center, Leiden, The Netherlands

<sup>2</sup> Department of Radiation Science & Technology, Delft University of Technology, Delft, The Netherlands

<sup>3</sup> Department of Radiology, Leiden University Medical Center, Leiden, The Netherlands

<sup>4</sup> Biomedical Photonic Imaging Group, University of Twente, Enschede, The Netherlands

<sup>5</sup> Department of Pathology, Leiden University Medical Center, Leiden, The Netherlands

<sup>6</sup> Centre for Human Drug Research, Leiden, The Netherlands

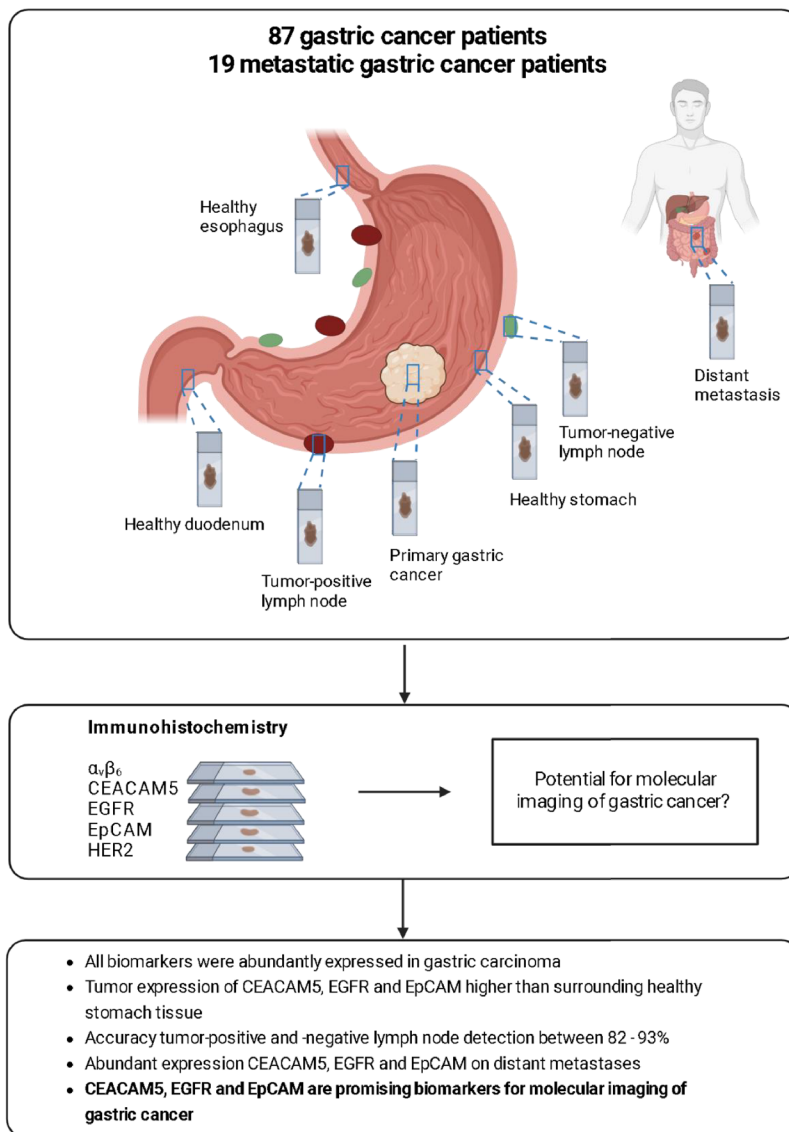
## Graphical Abstract

## Molecular Diagnosis &amp; Therapy

PEER-REVIEWED  
FEATURE

## Selecting Targets for Molecular Imaging of Gastric Cancer: an Immunohistochemical Evaluation

Ruben D. Houvast, Maurice van Duijvenvoorde, Kira Thijse, Wobbe O. de Steur, Lioe-Fee de Geus-Oei, A. Stijn. L. P. Crobach, Jacobus Burggraaf, Alexander L. Vahrmeijer, Peter J.K. Kuppen



This graphical abstract represents the opinions of the authors. For a full list of declarations, including funding and author disclosure statements, and copyright information, please see the full text online.

# 1 Introduction

Gastric cancer is the fifth most common malignancy, with a worldwide incidence of more than 1 million cases per year. Despite recent therapeutic advances, prognosis remains poor, with a 5-year survival of approximately 40%, resulting in more than 700,000 deaths worldwide annually [1, 2]. Achieving local control through subtotal or total gastrectomy combined with lymphadenectomy remains the cornerstone of multidisciplinary gastric cancer treatment [3]. Preoperatively, adequate disease staging is pivotal for patient-tailored treatment selection and maximizing its efficacy.

Preoperative work-up of gastric cancers is comprised of endoscopy, computed tomography (CT) imaging,  $^{18}\text{F}$ -fluorodeoxyglucose positron emission tomography ( $^{18}\text{F}$ -FDG PET) and/or diagnostic laparoscopy in clinically curable locally advanced disease ( $>cT3$  and/or  $N+$ ,  $M0$ ) [4, 5]. However, each modality has its limitations for accurate tumor detection, potentially leading to erroneous tumor staging and, consequently, unnecessary tumor resections, futile biopsies, extra imaging procedures and/or unnecessary administration of systemic therapy. For example, CT imaging provides accurate T-staging (sensitivity 83–100% for tumors with serosal involvement), while sensitivity for N-staging is lower at approximately 60% [4, 6, 7]. Importantly, sensitivity for small-sized distant metastases and peritoneal metastases is limited at 23–76%. Also, a significant proportion of gastric cancers have absent  $^{18}\text{F}$ -FDG PET avidity ( $\approx 20\%$ ), and non-specific uptake in the stomach wall can also mask tumor presence [5, 8]. The use of  $^{18}\text{F}$ -FDG PET for nodal and distant metastasis staging is also unsatisfactory, with sensitivity of 49% and 33–56%, respectively [5, 9].

To improve the accuracy of gastric cancer staging, diagnostic laparoscopy with or without peritoneal cytology is frequently performed [5, 10–12]. A systematic review highlighted that 9–60% of patients who were preoperatively staged as  $M0$  had irresectable disease intraoperatively [10]. Recently, the PLASTIC trial reported the limited added value of  $^{18}\text{F}$ -FDG PET and showed the superiority of diagnostic laparoscopy in accurate staging of locally advanced gastric cancer [5]. Limitations of laparoscopy, however, include its invasiveness, inability to accurately identify non-superficial liver metastases, lymph node metastases or extraperitoneal lesions, and the absence of tactile feedback for identifying malignant tissue [13, 14]. Besides tumor staging, an intraoperative challenge is encountered when radical resection is considered feasible. Studies showed that the presence of microscopically tumor-positive resection margins (i.e.,  $R1$  resection) is still observed in approximately 7% of gastric cancer patients, which has been associated with higher peritoneal recurrence rates and poorer survival [15, 16].

To address these challenges, tumor-targeted positron emission tomography (PET) and real-time fluorescence-guided surgery (FGS) using near-infrared light have emerged as valuable tools to enhance tumor imaging, respectively, by providing high-contrast visualization of malignant tissue [14, 17, 18]. These molecular imaging technologies could improve assessment of tumor localization, potentially avoiding resection for irresectable disease, as well as assisting surgeons in radical tumor resection. However, the success of molecular imaging hinges on the adequate selection of tumor-specific targets.

An ideal molecular imaging target is abundantly and homogeneously expressed on the tumor cell membrane across all patients, while expression in healthy surrounding tissue is absent [17]. Preferably, the target-of-interest is also present on lymph node and distant metastases and its expression remains present in microscopic residual disease after neoadjuvant therapy (NAT). However, governed by tumor heterogeneity, among others, a universal molecular imaging target for gastric cancer has still not been identified.

Over the last years, several targets were recognized as promising for molecular imaging of gastrointestinal cancers, including integrin  $\alpha_v\beta_6$ , carcinoembryonic antigen-related cell adhesion molecule 5 (CEACAM5), epidermal growth factor receptor (EGFR), epithelial cell adhesion molecule (EpCAM) and human epidermal growth factor receptor-2 (HER2) [19–24]. Consequently, tracers targeting some of these biomarkers were evaluated in clinical trials for various gastrointestinal tumor types [25–30]. However, their potential for molecular imaging of gastric cancer has been underexplored.

This study, therefore, provides the first crucial step towards application of these tracers in gastric cancer, by evaluating  $\alpha_v\beta_6$ , CEACAM5, EGFR, EpCAM and HER2 as molecular imaging targets for gastric cancer and its metastases. To accomplish this, biomarker expression was evaluated within the full anatomical context of gastric cancer. Biomarker expression was, therefore, determined using immunohistochemistry on human tissue specimens of primary tumors, healthy surrounding stomach tissue, but also on esophageal and duodenal tissue, and  $LN^+$  and  $LN^-$ , and distant metastases.

## 2 Materials and Methods

### 2.1 Patient and Tissue Specimen Selection

Pathology reports of patients who underwent resection for gastric adenocarcinoma at the Leiden University Medical Center (LUMC) from 2013 to 2020 were retrospectively reviewed. Representative formalin-fixed paraffin-embedded (FFPE) tissue blocks and hematoxylin and eosin (HE) slides

of 87 patients, containing primary gastric tumor, healthy stomach, esophageal, duodenal and/or (metastatic) lymph node tissue, were selected and obtained from the biobank at the LUMC. To allow proper subgroup analyses, the cohort was constituted to contain approximately a 1:1 ratio of patients with diffuse and intestinal type tumors according to the Laurén classification. Patients with mixed type Laurén classification were excluded. Selection of FFPE tissue blocks was performed by a gastrointestinal pathologist (ASLPC) based on the HE slides. Tissue specimens containing gastric adenocarcinoma metastases biopsy tissue were also obtained from 19 patients. Clinicopathological data were obtained from patients' medical records. Pathological tumor (pT) and pathological lymph node (pN) stages were defined according to the 8<sup>th</sup> edition of the American Joint Committee on Cancer and Union for International Cancer Control (AJCC/UICC) TNM staging system for gastric cancer. The study protocol was approved by both the Gastroenterology Biobank Review Committee (protocol reference: 2020-16) as well as the local medical ethical review committee (protocol reference: B20.052). This study was conducted in compliance with the Dutch code of conduct for responsible use of human tissue in medical research. Tissue specimens and clinicopathological data were handled in an anonymized manner and in compliance with the Declaration of Helsinki (1964).

## 2.2 Immunohistochemistry

Tissue sections 4 µm thick and cut from FFPE tissues were mounted on glass slides. Sections underwent deparaffinization in xylene for 15 min, followed by rehydration through sequential ethanol concentrations (100%, 50% and 25%). Subsequently, endogenous peroxidase was blocked using a 0.3% hydrogen peroxide solution. Antigen retrieval was tailored to the primary antibody employed, as outlined in Supplementary Table 1 in the electronic supplementary material (ESM). Post-antigen retrieval, slides were thoroughly rinsed in phosphate-buffered saline (PBS, pH 7.4). Primary antibodies (see Supplementary Table 1 in the ESM) targeting  $\alpha_v\beta_6$ , CEACAM5, EGFR, EpCAM or HER2 were applied to the tissue sections, which were subsequently left to incubate overnight at room temperature in a humid incubator. After overnight incubation, slides were rinsed in PBS to remove any residual primary antibodies. Anti-mouse horseradish peroxidase (HRP) or anti-rabbit HRP secondary antibodies (Envision, Dako, Glostrup, Denmark) were subsequently applied for 30 min at room temperature in a humid incubator for 30 min. Secondary antibodies were then removed by thorough PBS rinsing. Visualization of antibody binding was achieved using a 3,3'-diaminobenzidine (DAB) tetrahydrochloride solution (K3468, Agilent Technologies, Inc., Santa Clara, CA, USA) for 10 min at room temperature. Finally,

slides were counterstained with Mayer's hematoxylin (Klinipath B.V., Olen, Belgium), dehydrated in a dry incubator for 2 h and mounted using Pertex (Leica Microsystems, Wetzlar, Germany).

## 2.3 Evaluation of Immunohistochemical Staining

Whole slide images of the stained tissue slides were captured using the PANNORAMIC<sup>®</sup> 250 Flash III DX scanner (3DHISTECH Ltd, Budapest, Hungary). DAB staining was quantified using the total immunostaining score (TIS), which was computed by multiplying the staining proportion ( $0 = \leq 9\%$ ,  $1 = 10\text{--}25\%$ ,  $2 = 26\text{--}50\%$ ,  $3 = 51\text{--}75\%$ ,  $4 = \geq 76\%$ ) by the staining intensity ( $0 = \text{none}$ ,  $1 = \text{weak}$ ,  $2 = \text{moderate}$ ,  $3 = \text{strong}$ ). Staining based on the TIS was categorized as follows:  $0 = \text{negative}$ ;  $1, 2, 3, 4 = \text{weak expression}$ ;  $6, 8 = \text{moderate expression}$ ;  $9, 12 = \text{strong expression}$ . A panel of three independent observers (RDH, MvD, ASLPC) conducted the scoring. Instances of disagreement were discussed in a consensus meeting, during which the final score was conclusively determined.

## 2.4 Statistical Analysis

For categorical data, groups at baseline were compared using a Chi-square test. An independent samples *t* test was used to compare continuous variables of patient characteristics. TIS values between tumor, healthy surrounding stomach, esophageal and duodenal tissue were compared using Kruskal-Wallis test with Dunn's correction for multiple comparisons. Biomarker expression subgroup analyses were performed using a Mann-Whitney test. IBM SPSS statistics version 29 (IBM Corporation, Armonk, NY, USA) was used for all statistical analyses of patient characteristics. Graphs and statistical analyses for biomarker expression were created and performed using GraphPad Prism version 8 (GraphPad Software, La Jolla, CA, USA). Differences with a *p* value < 0.05 were considered significant.

# 3 Results

## 3.1 Patient Characteristics

Eighty-seven patients diagnosed with gastric adenocarcinoma were included, of which 45 (52%) had diffuse type disease and 42 (48%) had intestinal type disease. Clinicopathological characteristics are summarized in Table 1. In the intestinal type group, 17 patients (40%) had well-moderately differentiated tumors, compared to 0 (0%) in the diffuse type group ( $p < 0.001$ ). NAT consisted of chemotherapy, while one patient received chemoradiotherapy. Albeit not statistically significant, there was a small

difference in the number of patients who received NAT in both groups (diffuse type: 32 [71%]; intestinal type: 22 [52%];  $p = 0.097$ ). Other baseline characteristics did not differ between both groups.

### 3.2 Biomarker Expression in Primary Gastric Cancer Tissue Specimens

Tissue slides were stained for  $\alpha_v\beta_6$ , CEACAM5, EGFR, EpCAM and HER2 expression, and expression was quantified using the TIS. Representative examples of these stainings are shown in Fig. 1. Positive expression (TIS values  $\geq 1$ ) on primary gastric tumors was found in 86% of the tumors

for  $\alpha_v\beta_6$ , 72% for CEACAM5, 77% for EGFR, 93% for EpCAM and 71% for HER2 (Table 2). Categorized staining intensities are depicted in Table 3. All biomarkers showed a membranous staining pattern, with  $\alpha_v\beta_6$  and EpCAM showing a mostly homogenous staining pattern, while staining was slightly more heterogeneous for CEACAM5, EGFR and HER2 (Fig. 1). Additionally, biomarker co-expression in primary gastric tumors was analyzed (Table 4). The highest co-expressing biomarker combination was  $\alpha_v\beta_6$  and EpCAM, which were simultaneously expressed in 84% for primary gastric tumors. The remaining biomarker combinations were always expressed in more than 55% of cases, indicating moderate co-expression. Additionally, for all biomarker

**Table 1** Patient characteristics of the total gastric cancer cohort ( $n = 87$ ) as well as diffuse type ( $n = 45$ ) and intestinal type ( $n = 42$ ) subgroups

| Characteristic                 | Total ( $n = 87$ ) | Diffuse type ( $n = 45$ ) | Intestinal type ( $n = 42$ ) | $P$ value |
|--------------------------------|--------------------|---------------------------|------------------------------|-----------|
| Age, mean (SD)                 | 67.2 (12.7)        | 64.3 (14.1)               | 70.3 (10.3)                  | 0.073     |
| Gender, $n$ (%)                |                    |                           |                              | 0.038     |
| Male                           | 28 (32)            | 26 (58)                   | 33 (79)                      |           |
| Female                         | 59 (68)            | 19 (42)                   | 9 (21)                       |           |
| Surgery type, $n$ (%)          |                    |                           |                              | 0.407     |
| Total gastrectomy              | 35 (40)            | 20 (44)                   | 15 (36)                      |           |
| Partial gastrectomy            | 52 (60)            | 25 (56)                   | 27 (64)                      |           |
| Tumor localization, $n$ (%)    |                    |                           |                              | 0.298     |
| Cardia/fundus                  | 15 (17)            | 6 (13)                    | 9 (21)                       |           |
| Corpus                         | 24 (28)            | 11 (24)                   | 13 (31)                      |           |
| Antrum                         | 34 (39)            | 20 (44)                   | 14 (33)                      |           |
| Pre-pyloric                    | 8 (9)              | 3 (7)                     | 5 (12)                       |           |
| Other                          | 6 (7)              | 5 (11)                    | 1 (2)                        |           |
| Tumor differentiation, $n$ (%) |                    |                           |                              | < 0.001   |
| Well-moderate                  | 17 (20)            | 0 (0)                     | 17 (40)                      |           |
| Poor                           | 51 (59)            | 27 (60)                   | 24 (57)                      |           |
| Missing                        | 19 (22)            | 18 (40)                   | 1 (2)                        |           |
| Primary tumor, $n$ (%)         |                    |                           |                              | 0.210     |
| pT1                            | 15 (17)            | 5 (11)                    | 10 (24)                      |           |
| pT2                            | 9 (10)             | 7 (16)                    | 2 (5)                        |           |
| pT3                            | 37 (43)            | 19 (42)                   | 18 (43)                      |           |
| pT4                            | 26 (30)            | 14 (31)                   | 12 (29)                      |           |
| Regional lymph nodes, $n$ (%)  |                    |                           |                              | 0.789     |
| pN0                            | 27 (31)            | 15 (33)                   | 12 (29)                      |           |
| pN1                            | 21 (24)            | 12 (27)                   | 9 (21)                       |           |
| pN2                            | 16 (18)            | 8 (18)                    | 8 (19)                       |           |
| pN3                            | 23 (26)            | 10 (22)                   | 13 (31)                      |           |
| Neoadjuvant therapy, $n$ (%)   |                    |                           |                              | 0.097     |
| Yes, chemotherapy              | 53 (61)            | 32 (71)                   | 21 (50)                      |           |
| Yes, chemoradiotherapy         | 1 (1)              | 0 (0)                     | 1 (2)                        |           |
| No                             | 33 (38)            | 13 (29)                   | 20 (48)                      |           |
| R-status, $n$ (%)              |                    |                           |                              | 0.234     |
| R0                             | 76 (87)            | 38 (84)                   | 38 (90)                      |           |
| R1                             | 10 (11)            | 7 (16)                    | 3 (7)                        |           |
| Missing                        | 1 (1)              | 0 (0)                     | 1 (2)                        |           |



combinations, 88–98% of primary tumors were positive for at least one of the two biomarkers ( $\geq 1$ ).

### 3.3 Subgroup Analyses of Biomarker Expression in Primary Gastric Cancer Tissue Specimens

Subgroup analyses revealed that median expression between diffuse and intestinal type tumors did not differ for all biomarkers except for HER2, which showed a lower median TIS on diffuse type tumors (median TIS 4.0 vs. 2.0,  $p = 0.0004$ ; also see Supplementary Table 2 in the ESM). Moreover, subgroup analyses of biomarker expression in primary tumor tissues between patients who did not receive NAT and those who received NAT revealed that the median TIS for CEACAM5 and EGFR was lower on tumor specimens derived from patients who received NAT (CEACAM5: median TIS 9.0 vs. 3.5,  $p = 0.0215$ ; EGFR: median TIS 6.0 vs. 3.0,  $p = 0.0072$ ; also see Supplementary Table 3 in the ESM). For the remaining biomarkers, primary tumor expression was similar in patients who received NAT and patients who did not receive NAT.

### 3.4 Biomarker Expression in Primary Gastric Cancer Versus Healthy Surrounding Stomach, Esophageal and Duodenal Tissue Specimens

Images of sequential tumor sections showing biomarker expression in primary gastric cancer and healthy surrounding stomach, esophageal and duodenal tissue specimens are shown in Fig. 1. Quantified TIS values representing expression of  $\alpha_v\beta_6$ , CEACAM5, EGFR, EpCAM and HER2 as well as the statistical comparison of biomarker expression is depicted in Fig. 2 and Supplementary Table 4 in the ESM. For  $\alpha_v\beta_6$ , median expression in primary gastric cancer tissue was lower compared to healthy surrounding stomach (median TIS 6.0 vs. 9.0,  $p < 0.0001$ ) and duodenal tissue (median TIS 6.0 vs. 9.0,  $p = 0.0427$ ), and similar to expression in esophageal tissue (median TIS 6.0 vs. 8.5,  $p > 0.9999$ ). For CEACAM5, expression in primary tumor tissue was higher compared to healthy surrounding stomach (median TIS 4.0 vs. 0.0,  $p < 0.0001$ ) and duodenal tissue (median TIS 4.0 vs. 0.0,  $p = 0.0003$ ), but comparable to esophageal tissue (median TIS 4.0 vs. 4.0,  $p > 0.9999$ ). EGFR expression in primary tumor tissue was higher compared to healthy surrounding stomach tissue (median TIS 4.0 vs. 2.0,  $p = 0.0023$ ) but similar to esophageal (median TIS 4.0 vs. 6.0,  $p = 0.2235$ ) and duodenal tissue (median TIS 4.0 vs. 3.0,  $p > 0.9999$ ). EpCAM expression in tumor tissue was higher compared to healthy surround stomach (median TIS 9.0 vs. 0.0,  $p < 0.0001$ ) and esophageal tissue (median TIS 9.0 vs. 0.0,  $p < 0.0001$ ), but comparable to expression in duodenal tissue (median TIS 9.0 vs. 6.0,  $p = 0.7003$ ). Lastly, HER2 expression in primary tumor tissue was not different from healthy surrounding stomach (median TIS 2.0 vs. 2.5,

$p > 0.9999$ ) and esophageal tissue (median TIS 2.0 vs. 5.0,  $p = 0.1454$ ) and lower than duodenal tissue (median TIS 2.0 vs. 8.0,  $p = 0.0152$ ).

### 3.5 Expression of Biomarkers in Tumor-Positive and Tumor-Negative Lymph Node Tissue Specimens

Biomarker expression was evaluated on metastatic lymph nodes (LN<sup>+</sup>) and tumor-negative lymph nodes (LN<sup>-</sup>). Representative immunohistochemical (IHC) images showing expression of  $\alpha_v\beta_6$ , CEACAM5, EGFR, EpCAM and HER2 on LN<sup>+</sup> tissue are shown in Fig. 3. Sensitivity, specificity, positive predictive value, negative predictive value and area under the curve were calculated based on dichotomous (positive/negative) biomarker expression and are depicted in Table 5. Although sensitivity for LN<sup>+</sup> versus LN<sup>-</sup> differentiation was moderate for HER2 and CEACAM5 (both 56%), no false-positive staining was observed. For the remaining biomarkers, higher sensitivity (range 72–82%) and 100% specificity for differentiation between LN<sup>+</sup> and LN<sup>-</sup> were observed, indicating their potential to serve as targets for imaging of metastatic lymph nodes. Accuracy for identifying LN<sup>+</sup> and LN<sup>-</sup> ranged between 82% and 93% for all biomarkers.

### 3.6 Expression of Selected Biomarkers in Metastatic Gastric Cancer Tissue Specimens

Based on their tumor-specific expression pattern and accurate LN<sup>+</sup> detection potential, CEACAM5, EGFR and EpCAM were selected for further analysis of their expression in metastatic gastric cancer tissue specimens derived from 19 patients. Patient characteristics of this cohort are described in Supplementary Table 5 in the ESM. Tissue specimens were derived from various locations, with the most common locations including the abdominal wall (4/19, 21%), peritoneum (3/19, 16%) and large/small intestine (both 2/19, 11%). Representative IHC images of HE, CEACAM5, EGFR and EpCAM staining are depicted in Fig. 4. Positive biomarker expression in metastatic gastric cancer tissue specimens was observed in 94% for CEACAM5, 88% for EGFR and 95% for EpCAM (Table 6). As can be derived from Table 7, CEACAM5 and EpCAM staining was predominantly strong, while EGFR staining was somewhat weaker.

## 4 Discussion

Molecular imaging through tumor-targeted PET and FGS can address current limitations in pre- and intraoperative staging as well as resection margin assessment of gastric



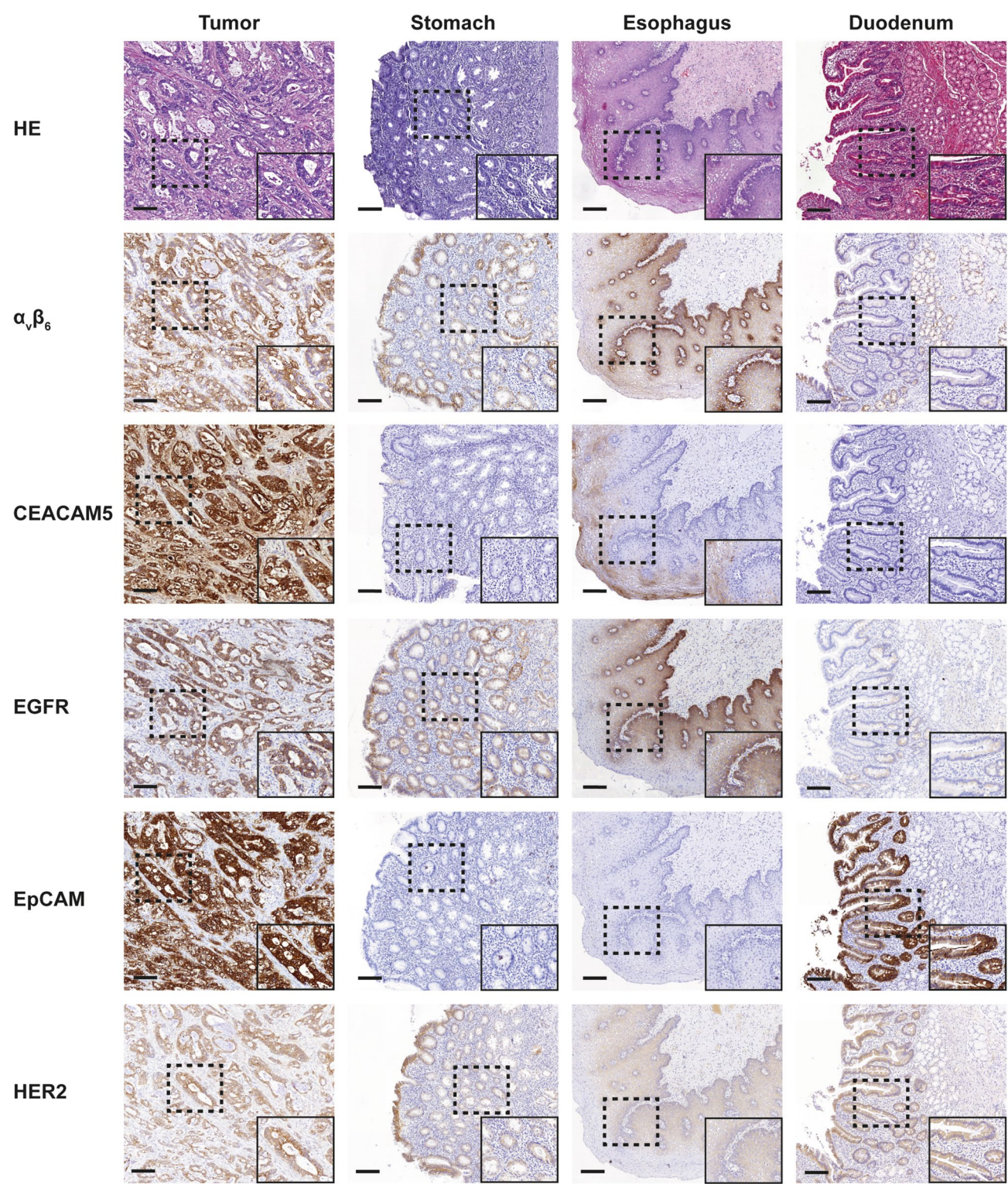


**Fig. 1** Representative images of HE and immunohistochemical staining of  $\alpha_v\beta_6$ , CEACAM5, EGFR, EpCAM and HER2 on primary gastric cancer, as well as healthy surrounding stomach, esophageal and duodenal tissue. Overview images and inserts are taken at 5 $\times$  and 20 $\times$  magnification, respectively. Scale bars represent 200  $\mu$ M.

CEACAM5 carcinoembryonic antigen-related cell adhesion molecule 5, EGFR epidermal growth factor receptor, EpCAM epithelial cell adhesion molecule, HE hematoxylin and eosin, HER2 human epidermal growth factor receptor-2



**Table 2** Percentages of positive biomarker expression in primary gastric cancer tissue specimens (TIS  $\geq 1$ )

| Biomarker         | Positive tumor expression (%) |
|-------------------|-------------------------------|
| $\alpha_v\beta_6$ | 86                            |
| CEACAM5           | 72                            |
| EGFR              | 77                            |
| EpCAM             | 93                            |
| HER2              | 71                            |

*CEACAM5* carcinoembryonic antigen-related cell adhesion molecule 5, *EGFR* epidermal growth factor receptor, *EpCAM* epithelial cell adhesion molecule, *HER2* human epidermal growth factor receptor-2, *TIS* total immunostaining score

cancer. Adequate selection and application of molecular imaging targets is the main prerequisite for adequate tumor visualization using these techniques. The current study showed that  $\alpha_v\beta_6$ , CEACAM5, EGFR, EpCAM and HER2, all promising tumor-specific targets for gastrointestinal cancers, were abundantly expressed in primary gastric tumor tissue specimens, with positive expression ranging

from 71% to 93%. Regarding biomarker co-expression, 88–98% of primary gastric tumors showed positive expression of at least one of two biomarkers for all possible biomarker combinations, indicating the potential added value of bispecific tracers to increase the number of patients eligible for molecular imaging. Additionally, CEACAM5, EGFR and EpCAM showed higher expression in tumor tissue compared to healthy surrounding stomach tissue, classifying these targets as suitable for primary gastric cancer imaging. As  $\alpha_v\beta_6$  and HER2 expression in healthy surrounding stomach tissue was higher or did not differ from primary tumor expression, respectively, we consider these targets not suitable for molecular imaging of primary gastric cancer. Despite moderate sensitivity for LN<sup>+</sup> detection observed for CEACAM5 and HER2 (both 56%), all biomarkers could distinguish LN<sup>+</sup> and LN<sup>-</sup> with high accuracy, indicating the potential of these targets for pre- and intraoperative N-staging. Lastly, EGFR, EpCAM and CEACAM5 showed moderate to strong expression in virtually all distant (peritoneal) metastases, highlighting their potential as targets for M-staging. Our study therefore demonstrated the feasibility of EGFR, EpCAM and

**Table 3** Distribution of  $\alpha_v\beta_6$ , CEACAM5, EGFR, EpCAM and HER2 expression on primary gastric cancer as quantified by the TIS values categorized into negative (TIS = 0), weak (TIS = 1, 2, 3, 4) moderate (TIS = 6, 8) or strong expression (TIS = 9, 12)

| Biomarker         | No. of tissue | Negative <i>n</i> (%) | Weak <i>n</i> (%) | Moderate <i>n</i> (%) | Strong <i>n</i> (%) |
|-------------------|---------------|-----------------------|-------------------|-----------------------|---------------------|
| $\alpha_v\beta_6$ | <i>n</i> = 87 | 12 (14)               | 27 (31)           | 24 (28)               | 24 (28)             |
| CEACAM5           | <i>n</i> = 87 | 24 (28)               | 20 (23)           | 14 (16)               | 29 (33)             |
| EGFR              | <i>n</i> = 84 | 19 (23)               | 26 (31)           | 26 (31)               | 13 (15)             |
| EpCAM             | <i>n</i> = 86 | 6 (7)                 | 7 (8)             | 18 (21)               | 55 (64)             |
| HER2              | <i>n</i> = 84 | 24 (29)               | 36 (43)           | 20 (24)               | 4 (5)               |

*CEACAM5* carcinoembryonic antigen-related cell adhesion molecule 5, *EGFR* epidermal growth factor receptor, *EpCAM* epithelial cell adhesion molecule, *HER2* human epidermal growth factor receptor-2, *TIS* total immunostaining score

**Table 4** Percentage of cases with positive  $\alpha_v\beta_6$ , CEACAM5, EGFR, EpCAM and HER2 expression for at least one of two biomarker combinations (panel:  $\geq 1$ ) along with the percentage of cases with positive expression of both biomarkers (panel: both), as quantified by a dichotomized TIS (TIS = 0: negative expression; all other TIS values: positive expression)

| Biomarker         | Panel    | $\alpha_v\beta_6$ (%) | CEACAM5 (%) | EGFR (%) | EpCAM (%) | HER2 (%) |
|-------------------|----------|-----------------------|-------------|----------|-----------|----------|
| $\alpha_v\beta_6$ | $\geq 1$ | –                     | 93          | 94       | 95        | 94       |
|                   | Both     | –                     | 66          | 77       | 84        | 71       |
| CEACAM5           | $\geq 1$ | 93                    | –           | 93       | 95        | 90       |
|                   | Both     | 66                    | –           | 56       | 70        | 55       |
| EGFR              | $\geq 1$ | 94                    | 93          | –        | 98        | 88       |
|                   | Both     | 77                    | 56          | –        | 74        | 59       |
| EpCAM             | $\geq 1$ | 95                    | 95          | 98       | –         | 94       |
|                   | Both     | 84                    | 70          | 74       | –         | 71       |
| HER2              | $\geq 1$ | 94                    | 90          | 88       | 94        | –        |
|                   | Both     | 71                    | 55          | 59       | 71        | –        |

*CEACAM5* carcinoembryonic antigen-related cell adhesion molecule 5, *EGFR* epidermal growth factor receptor, *EpCAM* epithelial cell adhesion molecule, *HER2* human epidermal growth factor receptor-2, *TIS* total immunostaining score

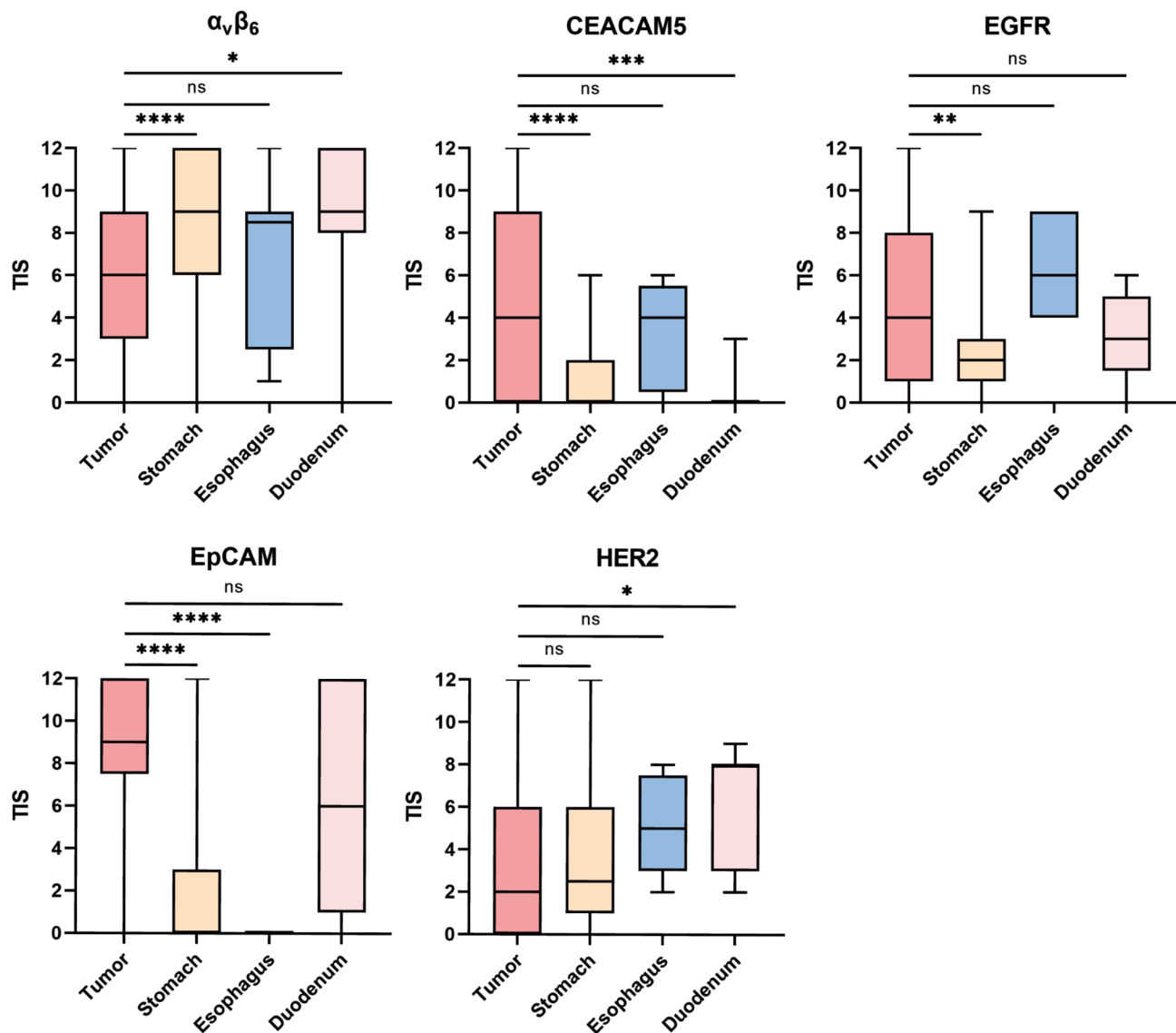


**Fig. 2** Box plots representing TIS values of  $\alpha_v\beta_6$ , CEACAM5, EGFR, EpCAM and HER2 staining on primary gastric cancer, as well as healthy surrounding stomach, esophageal and duodenal tissue. Horizontal lines represent the median TIS values, boxes represent interquartile range and brackets represent total TIS range. CEACAM5

carcinoembryonic antigen-related cell adhesion molecule 5, EGFR epidermal growth factor receptor, EpCAM epithelial cell adhesion molecule, HER2 human epidermal growth factor receptor-2, ns not significant, TIS total immunostaining score. \*  $p \leq 0.05$ , \*\*  $p \leq 0.01$ , \*\*\*  $p \leq 0.001$ , \*\*\*\*  $p \leq 0.0001$

CEACAM5 as molecular imaging targets for gastric cancer in a clinically relevant context.

The abundant tumor expression of the biomarkers reported herein is largely in line with previous studies, albeit we reported higher percentages of positive IHC staining compared to previous research, particularly for  $\alpha_v\beta_6$ , EGFR and HER2 [31–35]. This could, among others, have been caused by the use of different scoring systems, primary antibodies or antigen retrieval techniques during IHC staining, as well as inter- and intratumoral heterogeneity, and the relatively small sample sizes of previous IHC studies [36]. Confirmation of our results in a different or larger cohort of

gastric cancer patients could verify validity of the results observed herein, as well as elucidate underlying mechanisms contributing to these discrepancies.

A strong methodological point of this study is the additional evaluation of biomarker expression in healthy surrounding esophageal and duodenal tissue specimens. Similar CEACAM5 and EpCAM expression levels were found on healthy esophageal and duodenal tissue compared to tumor expression, respectively, while EGFR expression in both tissue types did not differ from tumor expression. Consistent with our findings, expression of CEACAM5 and EGFR has been identified in healthy esophageal tissue,

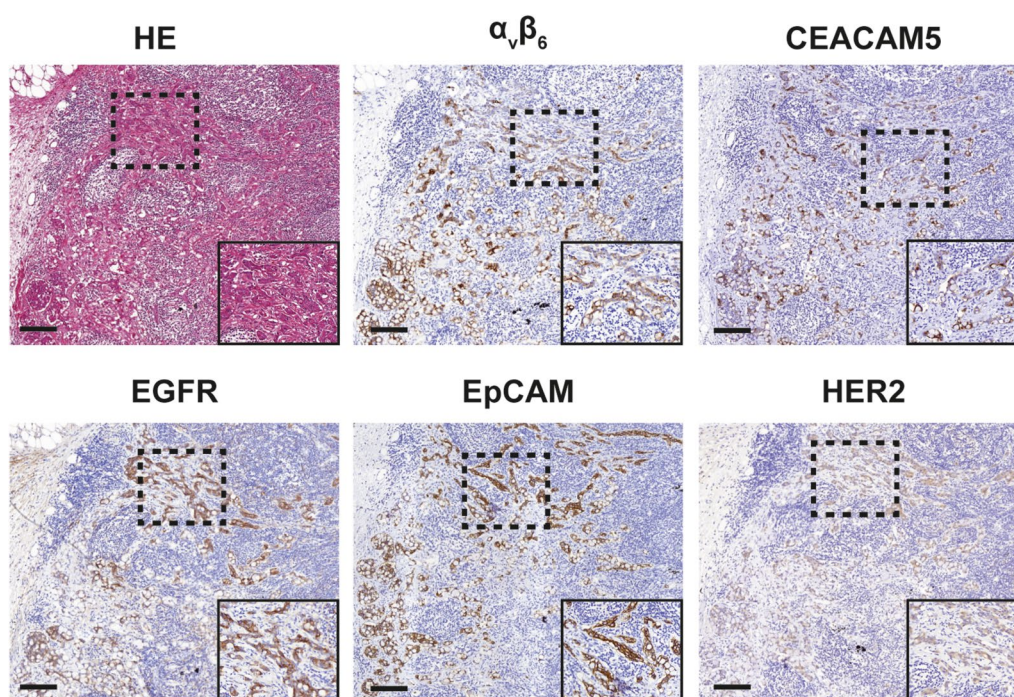


**Fig. 3** Representative images of HE and immunohistochemical staining of  $\alpha_v\beta_6$ , CEACAM5, EGFR, EpCAM and HER2 on lymph node metastases of gastric cancer. Overview images and inserts are taken at 5 $\times$  and 20 $\times$  magnification, respectively. Scale bars represent 200

$\mu\text{m}$ . CEACAM5 carcinoembryonic antigen-related cell adhesion molecule 5, EGFR epidermal growth factor receptor, EpCAM epithelial cell adhesion molecule, HE hematoxylin and eosin, HER2 human epidermal growth factor receptor-2

**Table 5** Sensitivity, specificity, PPV, NPV and accuracy along with the AUC and  $p$  value for identification of  $\text{LN}^+$  tissue specimens based on  $\alpha_v\beta_6$ , CEACAM5, EGFR, EpCAM and HER2 expression

| Biomarker         | Sens. (%) | Spec. (%) | PPV (%) | NPV (%) | Accuracy (%) | AUC (95% CI)        | $P$ value |
|-------------------|-----------|-----------|---------|---------|--------------|---------------------|-----------|
| $\alpha_v\beta_6$ | 72        | 100       | 100     | 85      | 89           | 0.860 (0.782–0.938) | < 0.0001  |
| CEACAM5           | 56        | 100       | 100     | 78      | 83           | 0.780 (0.689–0.872) | < 0.0001  |
| EGFR              | 74        | 100       | 100     | 86      | 90           | 0.872 (0.795–0.949) | < 0.0001  |
| EpCAM             | 82        | 100       | 100     | 89      | 93           | 0.908 (0.843–0.974) | < 0.0001  |
| HER2              | 56        | 100       | 100     | 77      | 82           | 0.780 (0.688–0.872) | < 0.0001  |

A dichotomized (positive/negative) TIS was used (TIS = 0: negative; all other TIS values: positive expression)

AUC area under the curve, CEACAM5 carcinoembryonic antigen-related cell adhesion molecule 5, CI confidence interval, EGFR epidermal growth factor receptor, EpCAM epithelial cell adhesion molecule, HER2 human epidermal growth factor receptor-2,  $\text{LN}^+$  tumor-positive lymph node, NPV negative predictive value, PPV positive predictive value, Sens. sensitivity, Spec. specificity, TIS total immunostaining score

while EGFR and EpCAM expression in, respectively, duodenal mucosa and epithelia of both the small and large intestines was also reported [21, 37–40]. Although previous literature described that EpCAM is overexpressed in gastrointestinal tumors compared to healthy surrounding tissue, it should be noted that EpCAM's presence in the small and large intestine might impact the detection of peritoneal metastases of gastric cancer using EpCAM-targeted molecular imaging tracers [21]. Taken further, the absence of EpCAM in esophageal tissue makes EpCAM a more suitable target for delineation of proximal gastric cancers

located near the esophageal-gastric junction (EGJ), while absence of CEACAM5 on duodenum epithelium makes this target appropriate for assessing resection margins of distal gastric cancers invading the duodenum. Of note, EGJ and duodenal invasion are frequently present in (sub)cardia (33–50%) and distal gastric cancer (14–33%), respectively [41–43]. Moreover, considering the increased R1 resection rate and reduced patient survival in these locally advanced cancers, adequate intraoperative tumor delineation may be a valuable tool to improve adequate

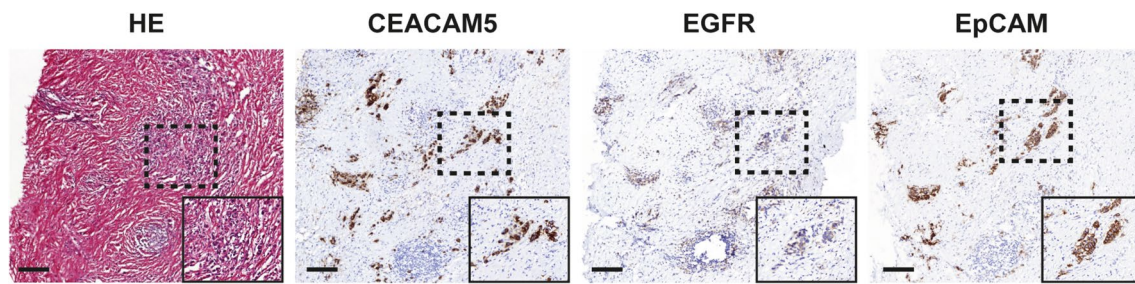


**Fig. 4** Representative images of HE and immunohistochemical staining of CEACAM5, EGFR and EpCAM on distant metastases of gastric cancer. Overview images and inserts are taken at 5× and 20× magnification, respectively. Scale bars represent 200 μm. *CEACAM5*

carcinoembryonic antigen-related cell adhesion molecule 5, *EGFR* epidermal growth factor receptor, *EpCAM* epithelial cell adhesion molecule, *HE* hematoxylin and eosin

**Table 6** Percentages of positive biomarker expression in metastatic gastric cancer tissue specimens (TIS ≥1)

| Biomarker | Positive tumor expression (%) |
|-----------|-------------------------------|
| CEACAM5   | 94                            |
| EGFR      | 88                            |
| EpCAM     | 95                            |

*CEACAM5* carcinoembryonic antigen-related cell adhesion molecule 5, *EGFR* epidermal growth factor receptor, *EpCAM* epithelial cell adhesion molecule, *TIS* total immunostaining score

resection margin assessment and, potentially, patient outcomes [44, 45].

In addition, the inclusion of patients with diffuse and intestinal type adenocarcinomas, as well as patients who received NAT, allowed subgroup analyses to study potential effect of these clinicopathological factors on the biomarkers' expression level. Interestingly, we found similar biomarker expression in diffuse and intestinal type adenocarcinomas for all biomarkers, except for HER2, which showed lower TIS values on intestinal type tumor tissue specimens. This makes the remaining biomarkers broadly applicable as molecular imaging markers in gastric cancer patients. Moreover, this finding is particularly promising for molecular imaging of diffuse type gastric cancers, given the lower  $^{18}\text{F}$ -FDG PET avidity, more frequent underestimation of the proximal

margin length and increased irradical resection rate in this histological subtype [44, 46–49]. Additionally, subgroup analyses revealed that CEACAM5 and EGFR expression was lower in patients who received NAT. Consequently, care should be taken when targeting CEACAM5 and EGFR for molecular imaging of primary gastric tumors after NAT.

Preoperatively, several targeted PET tracers have aimed to address current limitations in staging of gastric cancer in both the preclinical and clinical setting, with a strong focus on fibroblast activation protein (FAP)-targeted agents [18]. FAP is expressed in 55–75% of gastric carcinomas and is associated with increased migration, invasion and reduced survival, while expression in healthy surrounding tissues is virtually absent [50–52]. A recent meta-analysis showed that FAPI PET outperformed conventional  $^{18}\text{F}$ -FDG PET sensitivity for primary tumor, lymph node metastasis and peritoneal dissemination of gastric cancer, thereby indicating the potential of both FAPI PET and targeted PET in general [53, 54]. However, the overexpression of FAP in tissue during instances of tissue remodeling, such as wound healing or chronic inflammation, could pose a threat for its potential to delineate benign from malignant tissue [55]. Nevertheless, although our study intended to focus on tumor cell-specific molecular imaging targets, additional evaluation and comparison of FAP expression in our cohort would be an interesting continuation of this study.

**Table 7** Distribution of CEACAM5, EGFR and EpCAM expression in metastatic gastric cancer tissue specimens as quantified by the TIS values categorized into negative (TIS = 0), weak (TIS = 1, 2, 3, 4) moderate (TIS = 6, 8) or strong expression (TIS = 9, 12)

| Biomarker | No. of tissue | Negative <i>n</i> (%) | Weak <i>n</i> (%) | Moderate <i>n</i> (%) | Strong <i>n</i> (%) |
|-----------|---------------|-----------------------|-------------------|-----------------------|---------------------|
| CEACAM5   | <i>n</i> = 18 | 1 (6)                 | 6 (33)            | 4 (22)                | 7 (39)              |
| EGFR      | <i>n</i> = 16 | 2 (13)                | 10 (63)           | 2 (13)                | 2 (13)              |
| EpCAM     | <i>n</i> = 19 | 1 (5)                 | 3 (16)            | 2 (11)                | 13 (68)             |

*CEACAM5* carcinoembryonic antigen-related cell adhesion molecule 5, *EGFR* epidermal growth factor receptor, *EpCAM* epithelial cell adhesion molecule, *TIS* total immunostaining score



Of the targets evaluated herein, only HER2 has been clinically targeted for PET imaging in gastric cancer. Using  $^{89}\text{Zr}$ -trastuzumab, O'Donoghue et al. observed tumor accumulation in 80% of patients with positive HER2 status; however, not all known lesions could be visualized in these patients [56]. Interestingly, the authors did not observe significant stomach uptake as one would expect based on our observation of similar HER2 expression in primary tumors and healthy surrounding stomach tissue. It should be noted that, although positive biomarker expression remains a fundamental criterion for successful molecular imaging, it does not invariably correlate with positive tumor uptake in the clinical setting, underscoring the importance of both tumor heterogeneity and extensive clinical validation of molecular imaging tracers. Noteworthy, significant stomach wall and intestine uptake is commonly reported for  $\alpha_v\beta_6$ -targeting PET tracers, thus reflecting our findings of high  $\alpha_v\beta_6$  expression in these tissue types [57].

FGS-related research in gastric cancer has particularly focused on fluorescence-guided lymphadenectomy, as opposed to primary tumor imaging or intraoperative tumor staging. For instance, Chen et al. randomized gastric cancer patients between indocyanine green tracer-guided (ICG) lymphadenectomy using submucosal injection 1 day preoperatively and conventional laparoscopic gastrectomy [58]. The authors showed that ICG lymphadenectomy yielded more lymph nodes compared to the non-ICG group, leading to less unremoved lymph node stations, while complication rates between both groups were similar. However, sensitivity for metastatic lymph node detection was moderate at 56%. Considering these and previously outlined constraints in accurate intraoperative staging of gastric cancer staging, redirecting focus in FGS-related research towards tumor-targeted imaging could pave the way for novel tracers that address these limitations.

This study has some limitations. For instance, the relatively small sample size may have reduced the robustness of our subgroup analyses. Therefore, the findings of the subgroup analyses reported herein, although relevant for the assessment of a molecular imaging target's suitability, should be interpreted with caution. Secondly, due to the presence of staining artefacts, some slides were not suitable for scoring. Nevertheless, as the amount of excluded tissue slides per marker was limited (maximum 3/87 primary tumor specimens), we do not anticipate this influenced the findings of our study and the reproducibility thereof.

Future research into molecular imaging targets for gastric cancer could focus on their expression in premalignant tissue, such as chronic gastritis, intestinal metaplasia or dysplasia, thereby establishing the targets' potential for differentiation between malignant and benign tissue [59]. Also, as molecular targets are not expressed in all patients, preoperative screening for positive biomarker expression

could be performed, followed by application of the most suitable molecular imaging tracer. When feasible, such a strategy would form a robust and efficient way of patient-tailored employment of molecular imaging tracers in gastric cancer, maximizing its potential to improve pre- and intraoperative staging as well as resection margin assessment. This may be performed using biopsy material of primary gastric tumors or metastases, which is routinely obtained for histological diagnosis. Moreover, the predictive value of biomarker expression in tumor biopsies for primary gastric tumor expression remains to be elucidated.

## 5 Conclusion

Our findings show that CEACAM5, EGFR and EpCAM are promising targets for molecular imaging of gastric cancer, as well as lymph node and distant metastases. By improving pre- and intraoperative identification of tumor tissue, targeted PET and FGS could enhance gastric cancer staging and resection, ultimately leading to improved patient outcomes. Further clinical evaluation of PET and FGS tracers targeting these antigens is warranted.

**Supplementary Information** The online version contains supplementary material available at <https://doi.org/10.1007/s40291-024-00755-5>.

**Acknowledgements** We thank Ronald van Vlierberghe, Geeske Dekker-Ensink and Shadhvi Bhairosingh for their assistance during immunohistochemistry and tissue slide scanning. The graphical abstract was created using BioRender.com.

## Declarations

**Funding** No external funding was obtained for this study.

**Conflict of Interest** RDH, MvD, KT, WdS, LFdGO, ASLPC, JB, ALV and PJKK declare no conflict of interest.

**Availability of Data and Material** The data presented in this study are available upon reasonable request from the corresponding author.

**Ethics Approval** The study protocol was approved by both the Gastroenterology Biobank Review Committee (protocol reference: 2020-16) and the local medical ethical review committee (protocol reference: B20.052). This study was conducted in compliance with the Dutch code of conduct for responsible use of human tissue in medical research. Tissue specimens and clinicopathological data were handled in anonymized manner and in compliance with the Declaration of Helsinki (1964).

**Consent to Participate** The need for informed consent was waived by the local medical ethical review committee.

**Consent for Publication** Not applicable.

**Code Availability** Not applicable.

**Author Contributions** RDH was responsible for conceptualization, methodology, formal analysis and visualization, and wrote the original draft of the manuscript. KT and RDH conducted the immunohistochemical experiments, and RDH, MvD and ASLPC contributed to scoring of the immunohistochemical stainings. All remaining authors contributed to reviewing and editing the manuscript. PJKK supervised the study. All authors read and approved the final version of the manuscript.

**Open Access** This article is licensed under a Creative Commons Attribution-NonCommercial 4.0 International License, which permits any non-commercial use, sharing, adaptation, distribution and reproduction in any medium or format, as long as you give appropriate credit to the original author(s) and the source, provide a link to the Creative Commons licence, and indicate if changes were made. The images or other third party material in this article are included in the article's Creative Commons licence, unless indicated otherwise in a credit line to the material. If material is not included in the article's Creative Commons licence and your intended use is not permitted by statutory regulation or exceeds the permitted use, you will need to obtain permission directly from the copyright holder. To view a copy of this licence, visit <http://creativecommons.org/licenses/by-nc/4.0/>.

## References

- Li Y, Feng A, Zheng S, Chen C, Lyu J. Recent estimates and predictions of 5-year survival in patients with gastric cancer: a model-based period analysis. *Cancer Control*. 2022;29:10732748221099228. <https://doi.org/10.1177/10732748221099227>.
- Sung H, Ferlay J, Siegel RL, Laversanne M, Soerjomataram I, Jemal A, et al. Global cancer statistics 2020: GLOBOCAN Estimates of Incidence and Mortality Worldwide for 36 Cancers in 185 Countries. *CA Cancer J Clin*. 2021;71(3):209–49. <https://doi.org/10.3322/caac.21660>.
- Mocan L. Surgical management of gastric cancer: a systematic review. *J Clin Med*. 2021. <https://doi.org/10.3390/jcm10122557>.
- Borggreve AS, Goense L, Brenkman HJF, Mook S, Meijer GJ, Wessels FJ, et al. Imaging strategies in the management of gastric cancer: current role and future potential of MRI. *Br J Radiol*. 2019;92(1097):20181044. <https://doi.org/10.1259/bjr.20181044>.
- Gertsen EC, Brenkman HJF, van Hillegersberg R, van Sandick JW, van Berge Henegouwen MI, Gisbertz SS, et al. 18F-Fludeoxyglucose-positron emission tomography/computed tomography and laparoscopy for staging of locally advanced gastric cancer: a multicenter Prospective Dutch Cohort Study (PLASTIC). *JAMA Surg*. 2021;156(12): e215340. <https://doi.org/10.1001/jamasurg.2021.5340>.
- Giandola T, Maino C, Marrapodi G, Ratti M, Ragusi M, Bigioger V, et al. Imaging in gastric cancer: current practice and future perspectives. *Diagnostics (Basel)*. 2023. <https://doi.org/10.3390/diagnostics13071276>.
- Kim SH, Kim JJ, Lee JS, Kim SH, Kim BS, Maeng YH, et al. Preoperative N staging of gastric cancer by stomach protocol computed tomography. *J Gastric Cancer*. 2013;13(3):149–56. <https://doi.org/10.5230/jgc.2013.13.3.149>.
- Findlay JM, Antonowicz S, Segaran A, El Kafsi J, Zhang A, Bradley KM, et al. Routinely staging gastric cancer with (18)F-FDG PET-CT detects additional metastases and predicts early recurrence and death after surgery. *Eur Radiol*. 2019;29(5):2490–8. <https://doi.org/10.1007/s00330-018-5904-2>.
- Zhang Z, Zheng B, Chen W, Xiong H, Jiang C. Accuracy of (18) F-FDG PET/CT and CECT for primary staging and diagnosis of recurrent gastric cancer: a meta-analysis. *Exp Ther Med*. 2021;21(2):164. <https://doi.org/10.3892/etm.2020.9595>.
- Leake PA, Cardoso R, Seevaratnam R, Lourenco L, Helyer L, Mahar A, et al. A systematic review of the accuracy and indications for diagnostic laparoscopy prior to curative-intent resection of gastric cancer. *Gastric Cancer*. 2012;15(Suppl 1):S38–47. <https://doi.org/10.1007/s10120-011-0047-z>.
- Allen CJ, Blumenthaler AN, Das P, Minsky BD, Blum M, Roy-Chowdhuri S, et al. Staging laparoscopy and peritoneal cytology in patients with early stage gastric adenocarcinoma. *World J Surg Oncol*. 2020;18(1):39. <https://doi.org/10.1186/s12957-020-01813-y>.
- Fukagawa T. Role of staging laparoscopy for gastric cancer patients. *Ann Gastroenterol Surg*. 2019;3(5):496–505. <https://doi.org/10.1002/ags3.12283>.
- Schena CA, Laterza V, De Sio D, Quero G, Fiorillo C, Guna-wardena G, et al. The role of staging laparoscopy for gastric cancer patients: current evidence and future perspectives. *Cancers (Basel)*. 2023. <https://doi.org/10.3390/cancers15133425>.
- Vahrmeijer AL, Hutteman M, van der Vorst JR, van de Velde CJH, Frangioni JV. Image-guided cancer surgery using near-infrared fluorescence. *Nat Rev Clin Oncol*. 2013;10(9):507–18. <https://doi.org/10.1038/nrclinonc.2013.123>.
- Jiang Z, Liu C, Cai Z, Shen C, Yin Y, Yin X, et al. Impact of surgical margin status on survival in gastric cancer: a systematic review and meta-analysis. *Cancer Control*. 2021;28:10732748211043664. <https://doi.org/10.1177/10732748211043665>.
- Hirata Y, Agnes A, Estrella JS, Blum Murphy M, Das P, Minsky BD, et al. Clinical impact of positive surgical margins in gastric adenocarcinoma in the era of preoperative therapy. *Ann Surg Oncol*. 2023;30(8):4936–45. <https://doi.org/10.1245/s10434-023-13495-3>.
- Hernot S, van Manen L, Debie P, Mieog JSD, Vahrmeijer AL. Latest developments in molecular tracers for fluorescence image-guided cancer surgery. *Lancet Oncol*. 2019;20(7):e354–67. [https://doi.org/10.1016/S1470-2045\(19\)30317-1](https://doi.org/10.1016/S1470-2045(19)30317-1).
- Arçay Öztürk A, Flamen P. FAP-targeted PET imaging in gastrointestinal malignancies: a comprehensive review. *Cancer Imaging*. 2023;23(1):79. <https://doi.org/10.1186/s40644-023-00598-z>.
- de Geus SW, Boogerd LS, Swijnenburg RJ, Mieog JS, Tummers WS, Prevoo HA, et al. Selecting tumor-specific molecular targets in pancreatic adenocarcinoma: paving the way for image-guided pancreatic surgery. *Mol Imaging Biol*. 2016;18(6):807–19. <https://doi.org/10.1007/s11307-016-0959-4>.
- Tummers WS, Farina-Sarasqueta A, Boonstra MC, Prevoo HA, Sier CF, Mieog JS, et al. Selection of optimal molecular targets for tumor-specific imaging in pancreatic ductal adenocarcinoma. *Oncotarget*. 2017;8(34):56816–28. <https://doi.org/10.18632/oncotarget.18232>.
- Linders D, Deken M, van der Valk M, Tummers W, Bhairasingh S, Schaap D, et al. CEA, EpCAM, αvβ6 and uPAR expression in rectal cancer patients with a pathological complete response after neoadjuvant therapy. *Diagnostics (Basel)*. 2021. <https://doi.org/10.3390/diagnostics130516>.
- Wang L, Liang M, Xiao Y, Chen J, Mei C, Lin Y, et al. NIR-II navigation with an EGFR-targeted probe improves imaging resolution and sensitivity of detecting micrometastases in esophageal squamous cell carcinoma xenograft models. *Mol Pharm*. 2022;19(10):3563–75. <https://doi.org/10.1021/acs.molpharmaceut.2c00115>.
- Spizzo G, Fong D, Wurm M, Ensinger C, Obrist P, Hofer C, et al. EpCAM expression in primary tumour tissues and metastases: an immunohistochemical analysis. *J Clin Pathol*. 2011;64(5):415–20. <https://doi.org/10.1136/jcp.2011.090274>.

24. Yan M, Schwaederle M, Arguello D, Millis SZ, Gatalica Z, Kurzrock R. HER2 expression status in diverse cancers: review of results from 37,992 patients. *Cancer Metastasis Rev.* 2015;34(1):157–64. <https://doi.org/10.1007/s10555-015-9552-6>.
25. Hausner SH, Bold RJ, Cheuy LY, Chew HK, Daly ME, Davis RA, et al. Preclinical development and first-in-human imaging of the integrin  $\alpha(v)\beta(6)$  with [(18F)] $\alpha(v)\beta(6)$ -binding peptide in metastatic carcinoma. *Clin Cancer Res.* 2019;25(4):1206–15. <https://doi.org/10.1158/1078-0432.Ccr-18-2665>.
26. Boogerd LSF, Hoogstins CES, Schaap DP, Kusters M, Handgraaf HJM, van der Valk MJM, et al. Safety and effectiveness of SGM-101, a fluorescent antibody targeting carcinoembryonic antigen, for intraoperative detection of colorectal cancer: a dose-escalation pilot study. *Lancet Gastroenterol Hepatol.* 2018;3(3):181–91. [https://doi.org/10.1016/s2468-1253\(17\)30395-3](https://doi.org/10.1016/s2468-1253(17)30395-3).
27. de Valk KS, Deken MM, Schaap DP, Meijer RP, Boogerd LS, Hoogstins CE, et al. Dose-finding study of a CEA-targeting agent, SGM-101, for intraoperative fluorescence imaging of colorectal cancer. *Ann Surg Oncol.* 2021;28(3):1832–44. <https://doi.org/10.1245/s10434-020-09069-2>.
28. Bragina O, von Witting E, Garousi J, Zelchan R, Sandström M, Orlova A, et al. Phase I study of (99m)Tc-ADAPT6, a scaffold protein-based probe for visualization of HER2 expression in breast cancer. *J Nucl Med.* 2021;62(4):493–9. <https://doi.org/10.2967/jnumed.120.248799>.
29. Gabriëls RY, van Heijst LE, Hooghiemstra WTR, van der Waaij AM, Kats-Ugurlu G, Karrenbeld A, et al. Detection of early esophageal neoplastic barrett lesions with quantified fluorescence molecular endoscopy using cetuximab-800CW. *J Nucl Med.* 2023;64(5):803–8. <https://doi.org/10.2967/jnumed.122.264656>.
30. Voskuil FJ, de Jongh SJ, Hooghiemstra WTR, Linssen MD, Steinkamp PJ, de Visscher S, et al. Fluorescence-guided imaging for resection margin evaluation in head and neck cancer patients using cetuximab-800CW: a quantitative dose-escalation study. *Theranostics.* 2020;10(9):3994–4005. <https://doi.org/10.7150/thno.43227>.
31. Lian PL, Liu Z, Yang GY, Zhao R, Zhang ZY, Chen YG, et al. Integrin  $\alpha v \beta 6$  and matrix metalloproteinase 9 correlate with survival in gastric cancer. *World J Gastroenterol.* 2016;22(14):3852–9. <https://doi.org/10.3748/wjg.v22.i14.3852>.
32. Wang W, Seeruttun SR, Fang C, Chen J, Li Y, Liu Z, et al. Prognostic significance of carcinoembryonic antigen staining in cancer tissues of gastric cancer patients. *Ann Surg Oncol.* 2016;23(4):1244–51. <https://doi.org/10.1245/s10434-015-4981-6>.
33. Arienti C, Pignatta S, Tesi A. Epidermal growth factor receptor family and its role in gastric cancer. *Front Oncol.* 2019;9:1308. <https://doi.org/10.3389/fonc.2019.01308>.
34. Dai M, Yuan F, Fu C, Shen G, Hu S, Shen G. Relationship between epithelial cell adhesion molecule (EpCAM) overexpression and gastric cancer patients: a systematic review and meta-analysis. *PLoS ONE.* 2017;12(4): e0175357. <https://doi.org/10.1371/journal.pone.0175357>.
35. Boku N. HER2-positive gastric cancer. *Gastric Cancer.* 2014;17(1):1–12. <https://doi.org/10.1007/s10120-013-0252-z>.
36. Meyerholz DK, Beck AP. Principles and approaches for reproducible scoring of tissue stains in research. *Lab Invest.* 2018;98(7):844–55. <https://doi.org/10.1038/s41374-018-0057-0>.
37. Zhou J, Fan X, Chen N, Zhou F, Dong J, Nie Y, et al. Identification of CEACAM5 as a biomarker for prewarning and prognosis in gastric cancer. *J Histochem Cytochem.* 2015;63(12):922–30. <https://doi.org/10.1369/0022155415609098>.
38. Patriarca C, Macchi RM, Marschner AK, Mellstedt H. Epithelial cell adhesion molecule expression (CD326) in cancer: a short review. *Cancer Treat Rev.* 2012;38(1):68–75. <https://doi.org/10.1016/j.ctrv.2011.04.002>.
39. Shi W, Zhang S. Expression of epidermal growth factor receptor in human duodenal ulcer. *Hua Xi Yi Ke Da Xue Xue Bao.* 1997;28(3):280–3.
40. Abedi-Ardekani B, Dar NA, Mir MM, Zargar SA, Lone MM, Martel-Planche G, et al. Epidermal growth factor receptor (EGFR) mutations and expression in squamous cell carcinoma of the esophagus in central Asia. *BMC Cancer.* 2012;12:602. <https://doi.org/10.1186/1471-2407-12-602>.
41. Ito H, Inoue H, Odaka N, Satodate H, Suzuki M, Mukai S, et al. Comparison of clinicopathological characteristics in the patients with cardiac cancer with or without esophagogastric junctional invasion: a single-center retrospective cohort study. *Int J Surg Oncol.* 2013;2013: 189459. <https://doi.org/10.1155/2013/189459>.
42. Oh SE, Park S, Ahn S, An JY, Lee JH, Sohn TS, et al. Prognostic significance of esophagogastric junction invasion in patients with adenocarcinoma of the cardia or subcardia. *Cancers (Basel).* 2023. <https://doi.org/10.3390/cancers15061656>.
43. Kumagai K, Sano T, Hiki N, Nunobe S, Tsujiura M, Ida S, et al. Survival benefit of “D2-plus” gastrectomy in gastric cancer patients with duodenal invasion. *Gastric Cancer.* 2018;21(2):296–302. <https://doi.org/10.1007/s10120-017-0733-6>.
44. Bissolati M, Desio M, Rosa F, Rausei S, Marrelli D, Baiocchi GL, et al. Risk factor analysis for involvement of resection margins in gastric and esophagogastric junction cancer: an Italian multicenter study. *Gastric Cancer.* 2017;20(1):70–82. <https://doi.org/10.1007/s10120-015-0589-6>.
45. Kumazu Y, Hayashi T, Yoshikawa T, Yamada T, Hara K, Shimoda Y, et al. Risk factors analysis and stratification for microscopically positive resection margin in gastric cancer patients. *BMC Surg.* 2020;20(1):95. <https://doi.org/10.1186/s12893-020-00744-5>.
46. Smyth EC, Verheij M, Allum W, Cunningham D, Cervantes A, Arnold D. Gastric cancer: ESMO Clinical Practice Guidelines for diagnosis, treatment and follow-up. *Ann Oncol.* 2016;27(suppl 5):v38–49. <https://doi.org/10.1093/annonc/mdw350>.
47. Dondi F, Albano D, Giubbini R, Bertagna F. 18F-FDG PET and PET/CT for the evaluation of gastric signet ring cell carcinoma: a systematic review. *Nucl Med Commun.* 2021;42(12):1293–300. <https://doi.org/10.1097/mnm.0000000000001481>.
48. Watanabe A, Adamson H, Lim H, McFadden AF, McConnell YJ, Hamilton TD. Intraoperative frozen section analysis of margin status as a quality indicator in gastric cancer surgery. *J Surg Oncol.* 2023;127(1):66–72. <https://doi.org/10.1002/jso.27107>.
49. Berlth F, Kim WH, Choi JH, Park SH, Kong SH, Lee HJ, et al. Prognostic impact of frozen section investigation and extent of proximal safety margin in gastric cancer resection. *Ann Surg.* 2020;272(5):871–8. <https://doi.org/10.1097/sla.0000000000004266>.
50. Puré E, Blomberg R. Pro-tumorigenic roles of fibroblast activation protein in cancer: back to the basics. *Oncogene.* 2018;37(32):4343–57. <https://doi.org/10.1038/s41388-018-0275-3>.
51. Kalaei Z, Manafi-Farid R, Rashidi B, Kiani FK, Zarei A, Fathi M, et al. The Prognostic and therapeutic value and clinical implications of fibroblast activation protein- $\alpha$  as a novel biomarker in colorectal cancer. *Cell Commun Signal.* 2023;21(1):139. <https://doi.org/10.1186/s12964-023-01151-y>.
52. Wang RF, Zhang LH, Shan LH, Sun WG, Chai CC, Wu HM, et al. Effects of the fibroblast activation protein on the invasion and migration of gastric cancer. *Exp Mol Pathol.* 2013;95(3):350–6.
53. Hathi DK, Jones EF. (68)Ga FAPI PET/CT: tracer uptake in 28 different kinds of cancer. *Radiol Imaging Cancer.* 2019;1(1): e194003. <https://doi.org/10.1148/rycan.2019194003>.
54. Wang Y, Luo W, Li Y. [(68)Ga]Ga-FAPI-04 PET MRI/CT in the evaluation of gastric carcinomas compared with [(18)F]-FDG PET

- MRI/CT: a meta-analysis. *Eur J Med Res.* 2023;28(1):34. <https://doi.org/10.1186/s40001-023-00997-9>.
55. Kessler L, Ferdinandus J, Hirmas N, Zarrad F, Nader M, Kersting D, et al. Pitfalls and common findings in (68)Ga-FAPI PET: a pictorial analysis. *J Nucl Med.* 2022;63(6):890–6. <https://doi.org/10.2967/jnumed.121.262808>.
56. O'Donoghue JA, Lewis JS, Pandit-Taskar N, Fleming SE, Schöder H, Larson SM, et al. Pharmacokinetics, biodistribution, and radiation dosimetry for (89)Zr-trastuzumab in patients with esophago-gastric cancer. *J Nucl Med.* 2018;59(1):161–6. <https://doi.org/10.2967/jnumed.117.194555>.
57. Kossatz S, Beer AJ, Notni J. It's time to shift the paradigm: translation and clinical application of non- $\alpha$ v $\beta$ 3 integrin targeting radiopharmaceuticals. *Cancers (Basel).* 2021. <https://doi.org/10.3390/cancers13235958>.
58. Chen QY, Xie JW, Zhong Q, Wang JB, Lin JX, Lu J, et al. Safety and efficacy of indocyanine green tracer-guided lymph node dissection during laparoscopic radical gastrectomy in patients with gastric cancer: a randomized clinical trial. *JAMA Surg.* 2020;155(4):300–11. <https://doi.org/10.1001/jamasurg.2019.6033>.
59. Koulis A, Buckle A, Boussioutas A. Premalignant lesions and gastric cancer: current understanding. *World J Gastrointest Oncol.* 2019;11(9):665–78. <https://doi.org/10.4251/wjgo.v11.i9.665>.